Mouse primary T cell phosphoyrosine proteomics enabled by BOOST

Xien Yu Chua[1], Kenneth P. Callahan[2], Alijah A. Griffith[2], Tobias Hildebrandt[2], Guoping Fu[3], Mengzhou Hu[1], Renren Wen[3], Arthur R. Salomon[2,*]

1 *Department of Molecular Pharmacology, Physiology & Biotechnology, Brown University, Providence, RI, 02912*

2 *Department of Molecular Biology, Cell Biology & Biochemistry, Brown University, Providence, RI, 02912*

3 *Blood Research Institute, Blood Center of Wisconsin, Milwaukee, WI, 53226*
∗ *Corresponding Author*∗

E-mail: art@drsalomon.com

Abstract

The Broad Spectrum Optimization of Selective Triggering (BOOST) approach was recently developed to increase the quantitative depth of the tyrosine phosphoproteome by mass spectrometry-based proteomics. While BOOST has been demonstrated in the Jurkat T cell line, it has not been demonstrated in scarce mice primary T cells. Here, we show the first phosphotyrosine proteomics performed in mice primary T cells using BOOST. Using BOOST, we identified and precisely quantificatied more than 5000 unique pTyr peptides using only 1 mg of protein from stimulated primary T cells from mice. We further reveal the importance of the phase-constrained spectrum deconvolution method (ΦSDM) parameter on Orbitrap instruments that, when disabled, enhanced quantitation depth, accuracy, and precision in low-abundance samples. Using samples with contrived ratios, we find that disabling ΦSDM allows for up to a two

fold increase in the number of statistically significant intensity ratios while enabling ΦSDM degrades quantitation, especially in low-abundance samples.

Keywords:

- **Mice**
- **T cell**
- **BOOST**
- **TMT**
- **SH2 superbinder**
- **Phosphotyrosine proteomics**
- **Phase-constrained spectrum deconvolution method**

Introduction

Kinase signaling cascades regulate key cellular processes including growth, differentiation, and trancsriptional regulation. In T cells, binding of antigen-loaded peptide major histocompatibility complex on antigen-presenting cells to the T cell receptor (TCR) initiates early tyrosine kinase-mediated signaling, leading to serine/threonine kinase activation that regulate transcriptional activation.[1] Signal initiation from begins by recruitment of the Src family tyrosine kinases Lck and Fyn, which phosphorylate tyrosine residues in immunotyrosine activation motifs (ITAMs) on the intracellular domain of TCR complex subunits TCRζ, CD3ϵ, CD3δ, and CD3γ.[1,2] Next, the tyrosine kinase Zap70 binds to phosphorylated ITAMs, is itself phosphorylated by TCR proximal Lck, and directed toward substrates associated with the critical scaffolding protein linker for activation of T cells (LAT) by Lck.[3] Zap70 and another Lck-activated tyrosine protein kinase named Itk phosphorylate and activate

many LAT-associated proteins, culminating in serine/threonine kinase activation upstream of cytokine expression and actin cytoskeletal regulation. Despite the importance of tyrosine phosphorylation in the early stages of TCR signaling, tyrosine phosphorylation is scarce, accounting for less than 1% of all phosphorylation events.[4,5]

Due to the scarce nature of tyrosine phosphorylation, large-scale phosphotyrosine (pTyr) proteomic studies of TCR signaling in mice primary T cells are often impaired by low yield. Recently, Locard-Paulet et al. performed a phosphoproteomic study with 100 million antibody-stimulated $CD4^+$ T cells from mice per replicate using the pTyr-1000 pTyr enrichment kit. Using this approach, Locard-Paulet et al. identified a total of 254 unique pTyr sites from 786 unique pTyr peptides, which is comparable to phosphoproteomic studies of TCR and chimeric antigen receptor signaling in primary human T cells.[7–9] Phosphotyrosine-specific enrichment methods provide improved pTyr sequencing compared to general phosphopeptide enrichment strategies like immobilized metal affinity chromatography (IMAC) or titanium dioxide (TiO_2), which are more common in phosphoproteomic studies in primary T cells from mice.[10,11] One phosphoproteomic study of TCR signaling in mice using 20 million cells per replicate and IMAC phosphopeptide enrichment identified only 77 unique pTyr peptides,[12] whereas other studies studies report 1-2% (about 250 to 700) of their total yield as unique pTyr peptides using IMAC or TiO_2.[10,13] As demonstrated in Iwai et al., decreasing the number of cells and therefore the amount of protein input can severely limit pTyr quantitation depth in primary T cells from mice.

To increase the accuracy, precision, and reporducibility of pTyr quantitation in low protein input samples, both experimental and computational approaches are being developed. For example, recent improvements in pTyr enrichment reagents, namely the superbinder SH2 enrichment method,[14–19] have improved quantitation depth of the pTyr proteome.[20–22] Additionally, the use of isobaric labeling reagents like tandem mass tags (TMT) have allowed for accurate quantitation in multiplexed samples with a higher probability of identifying unique peptides compared to label-free quantitation.[23–28] To improve the spectral quality and speed

of acquiring TMT samples Fourier transfrom-mass spectrometers (FT-MS), instrument settings like the phase-constrained spectrum deconvolution method (ΦSDM) are available. By applying ΦSDM, FT spectra are deconvolved into frequency distributions, allowing for efficient extraction of the harmonic components of oscillating ions and ultimately achieving higher mass accuracy and resolution in shorter times.[29]

Recently, we combined the multiplexing capability of TMT, the selectivity of superbinder SH2, and the ability to inhibit tyrosine phosphatases *in vivo* to develop the broad-spectrum optimization of selective triggering (BOOST) method to increase pTyr quantitation depth in proteomics experiment.[20] During the development of BOOST we used Jurkat T cells, a model system for studying TCR signaling,[30] however we have not demonstrated the BOOST method in the more biologically relevant primary T cells from mice. Here, we demonstrate the first pTyr proteomics study in primary T cells from mice using the BOOST method. By using predetermined protein input amounts, we show that BOOST increases the sequencing depth of low abundance samples, yielding more than 5,000 unique pTyr peptides. We also show that acquiring samples using ΦSDM degrades quantitation in low-abundance samples. By using samples with contrived ratios, samples acquired with ΦSDM disabled have higher replicate reproducibility, are more accurate, and are more precise than equivalent samples acquired with ΦSDM enabled.

Materials and Methods

Stimulation of mice primary T cells

CD8+ thymocytes from B6 mice were harvested and blasted in cell culture using IL-2. Cells were rested in 1% BSA T cell media for 2 hours at 2×10^6 cells/ml prior to stimulation. To initiate T cell stimulation, 25 μg/mL α-CD3 antibody and 25 μg/mL streptavidin were added to the cells resuspended at 1×10^8 cells/ml for 5 minutes at 37°C. After 5 minutes of stimulation, cells were lysed with 1% (w/v) sodium dodecyl sulfate (SDS) in 100 mM

Tris-HCl (pH 7.6). Pervanadate treatment was performed by incubating cells with 500 μM PV (prepared by mixing equal volume of 1 mM sodium orthovanadate and 1 mM hydrogen peroxide) for 20 minutes at 37°C.

Sample processing

Lysate was applied through QIAshredder Mini Spin Column by centrifugation at 20,000×g at 37°C for 5 minutes. Protein concentration was determined using Pierce BCA Protein Assay (Thermo Fisher Scientific, 23225), after which it was reduced by 100 mM dithiothreitol at room temperature for 30 minutes. Lysate was subsequently processed and digested using the filter-aided sample preparation (FASP) method[31] as described previously. Digested peptides were collected and acidified by trifluoroacetic acid and desalted using Sep-Pak C18 Cartridge (Waters WAT020515) as described previously.[32] Desalted peptides were labeled using a Tandem Mass Tag as described previously.[20] TMT-labeled peptides were mixed and purified for phosphotyrosine peptides as described previously.[20]

Liquid chromatography tandem mass spectrometry

For offline basic (pH 10) fractionation, peptides were separated on a 100 mm × 1.0 mm Acquity BEH C18 column (Waters) using an UltiMate 3000 UHPLC system (ThermoFisher Scientific) with a 40-minute gradient from 1% to 40% Buffer Bbasic into 36 fractions, which are subsequently consolidated into 12 super-fractions (Buffer A_{basic} = 10 mM ammonium hydroxide in 99.5% (v/v) HPLC-grade water, 0.5% (v/v) HPLC-grade acetonitrile; Buffer B_{basic} = 10 mM ammonium hydroxide in 100% HPLC-grade acetonitrile). Each super-fraction was further separated on an in-line 150 mm × 75 μm reversed phase analytical column packed in-house with XSelect CSH C18 2.5 μm resin (Waters) using an UltiMate 3000 RSLCnano system (ThermoFisher Scientific), at a flow rate of 300 nL/min. Peptides were eluted using a 65-minute gradient from 5% to 30% Buffer B_{acidic}, followed by a 6-minute gradient 30% to 90% Buffer B_{acidic} (Buffer A_{acidic} = 0.1% (v/v) formic acid in 99.4%

(v/v) HPLC-grade water, 0.5% (v/v) HPLC-grade acetonitrile; Buffer B_{basic} = 0.1% (v/v) formic acid in 99.9% (v/v) HPLC-grade acetonitrile). Data was acquired in DDA mode on a Orbitrap Eclipse Tribrid mass spectrometer (ThermoFisher Scientific) with a positive spray voltage of 2.25 kV using multinotch TMT-MS3 settings.[33] Cycle time was set at 2.5 seconds. At the MS1 level scans, precursor ions (charge states $2-5$) acquired on the Orbitrap detector with the scan range of $400-1600$ m/z, 120,000 resolution, maximum injection time of 50 ms, automatic gain control (AGC) target of 800,000, and a dynamic exclusion time of 15 seconds. MS1 precursor ions were isolated on the quadrupole using an isolation window of 0.7 m/z for MS2 scans. MS2 scans were acquired in centroid mode on the ion trap detector on a scan range of $400-1400$ m/z via higher-energy dissociation (HCD, 33% energy) activation with an AGC target of 5000, maximum injection time of 75 ms. Using synchronous precursor selection (SPS),[33] 10 notches were further isolated on the quadrupole using an MS2 isolation window of 3 m/z for MS3 scans, which are acquired on the Orbitrap detector on a scan range of $100-500$ m/z in a mass resolution of 50,000 via HCD activation (55% energy) with a AGC target of 250,000 and maximum injection time of 150 ms in centroid mode.

Database Search Parameters and Acceptance Criteria for Identifications

Raw files were processed in MaxQuant[34] version 1.6.17.0 using the integrated peptide search engine Andromeda.[35] MS/MS spectra were searched against a mouse UniProt database (Mus musculus, last modified 12/01/2019) comprised of 55,412 forward protein sequences. False discovery rate (FDR) for peptide spectrum matches (PSM) was set at 1% using a reverse decoy database approach. Carbamidomethylation (cysteine) was set as fixed modification, whereas oxidation (methionine), acetylation (protein N-termini) and phosphorylation (serine, threonine, tyrosine) were set as variable modifications. Trypsin enzyme specificity was used with up to 2 missed cleavages. Main search peptide tolerance was set as 5 ppm, while FTMS and ITMS MS/MS match tolerances were set as 20 ppm and 0.5 Da, respectively. MS3

reporter ion mass tolerance was set at 3 mDa, using isotopic correction factors provided by the manufacturer (Lot UK291564, Lot UH283151).

Data Analysis & Code Availability

All analysis and data visualization were preformed on Ubuntu 20.04 LTS in the Windows Subsystem for Linux version 2 using Python 3.8.10 with the packages "Matplotlib" (Version 3.3.2), "SciPy" (Version 1.7.3), "pandas" (Version 1.2.3), "NumPy" (Version 1.19.2), "Biopython" (version 1.78), and "matplotlib-venn" (version 0.11.6) and is available in Supporting Folder 1. Analysis of unique PSMs was performed using the MaxQuant output file "evidence.txt" (Supporting Folder 2). Unique PSMs were defined by a non-redundant amino acid sequence (including posttranslational modifications), the charge state of the peptide, and the least number of missing values across all TMT channels. In the cases where redundancy was still present, we kept the peptide with the highest median reporter intensity. For assigning flanking sequences to each peptide and generating Supporting Figure 1, the MaxQuant output file "Phospho (STY)Sites.txt" (Supplementary Folder 2) was used. For determining previously annotated pTyr sites we used the PhosphoSitePlus® (www.phosphosite.org)[36] posttranslational modification database file "Phosphorylation_site_dataset.txt" (Supporting Folder 1). For general pathway annotation, we downloaded the files "wikipathways-20220110-gmt-Homo_sapiens.gmt" and "wikipathways-20220110-gmt-Mus_musculus.gmt" (Supporting Folder 1) from the community managed biological pathway database WikiPathways.[37] Before analysis, all peptides flagged as "potential contaminants" or "reverse hits" were removed, and reporter ions from the PV-treated sample (TMT126) and the Blank channel (TMT127N) were excluded from further analysis unless otherwise stated. Statistical significance between the mean corrected reporter intensities for 1.0 mg, 0.3 mg, and 0.1 mg protein input samples was determined using unpaired Student's T-tests to calculate p-values before correcting for multiple hypotheses (generating q-values) using the method of Benjamini & Hochberg.[38] For all comparisons, statistical significance was only attained for peptides where reporter

intensity values were present for all three replicates. In line with the previous literature, we did not impute or interpolate missing values at any point during data analysis.[20,21] To evaluate replicate reproducibility, we performed least squares linear regression[39] on pairwise comparisons between replicates for each protein input amount in a given experiment, removing peptides for which one or both replicates contained missing values. For all volcano plots, we plotted $-\log_{10}(q\text{-value})$ as a function of $\log_{10}(\text{Ratio of Mean pTyr Intensities})$ for comparisons between 1.0 mg and 0.1 mg, 1.0 mg and 0.3 mg, and 0.3 mg and 0.1 mg of protein input for each TMT mix. For cases where volcano plots were constructed for each portion of a Venn diagram, separate volcano plots for each overlapping portion were constructed using the reporter intensity data from each experiment. For BOOST Factor plots, only pTyr peptides with at least one reporter ion value were used, and we used the following equation to calculate BOOST Factor for each pTyr peptide:

$$\begin{aligned} \text{BOOST Factor} &= \frac{\text{Total reporter ion current}_{\text{BOOST}}}{\text{Total reporter ion current}_{\text{Experimental}}} \\ &\approx \frac{\text{1.0 mg PV intensity}}{\text{Sum}(1\text{mg}_{\text{R1-R3}} + 0.3\text{mg}_{\text{R1-R3}} + 0.1\text{mg}_{\text{R1-R3}})}. \end{aligned} \tag{1}$$

The results of all analysis are provided in Supporting Tables 1-6, including references to the identification number(s) for each peptide in the original MaxQuant output file(s).

Results

Experimental Design & Rationale

In this study, we sought to determine the feasibility of the recently developed BOOST method for pTyr proteomics in primary T cells from mice. In short, BOOST is a method used to increase the precursor ion triggering and fragmentation of pTyr-containing peptides using a pervanadate (PV) treated sample in multiplexed TMT experiments, thus increasing quantitation depth of low-abundance posttranslational modifications.[20] Our design is similar

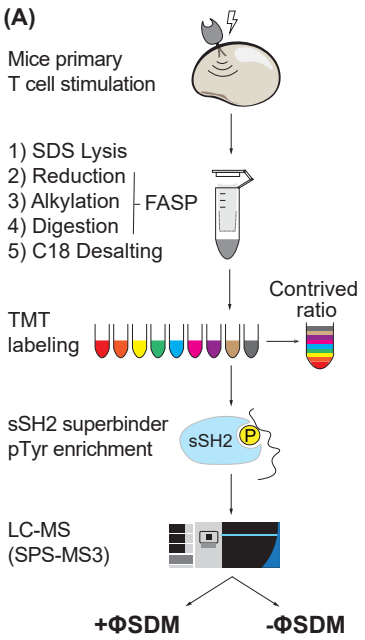

(B)

TMT	Control +ΦSDM	Control	BOOST +ΦSDM	BOOST
126	1 mg control	1 mg control	1 mg PV	1 mg PV
127N	1.0 mg Rep.1	1.0 mg Rep.1	1.0 mg Rep.1	1.0 mg Rep.1
127C	Blank	Blank	Blank	Blank
128N	1.0 mg Rep.2	1.0 mg Rep.2	1.0 mg Rep.2	1.0 mg Rep.2
128C	0.3 mg Rep.1	0.3 mg Rep.1	0.3 mg Rep.1	0.3 mg Rep.1
129N	1.0 mg Rep.3	1.0 mg Rep.3	1.0 mg Rep.3	1.0 mg Rep.3
129C	0.3 mg Rep.2	0.3 mg Rep.2	0.3 mg Rep.2	0.3 mg Rep.2
130N	0.1 mg Rep.1	0.1 mg Rep.1	0.1 mg Rep.1	0.1 mg Rep.1
130C	0.3 mg Rep.3	0.3 mg Rep.3	0.3 mg Rep.3	0.3 mg Rep.3
131N	0.1 mg Rep.2	0.1 mg Rep.2	0.1 mg Rep.2	0.1 mg Rep.2
131C	0.1 mg Rep.3	0.1 mg Rep.3	0.1 mg Rep.3	0.1 mg Rep.3

Figure 1: Schematic of (A) experimental workflow and (B) TMT mix and channel design.

to that of our previous BOOST studies,[20,21] using one 1.0 mg PV treated sample (or 1.0 mg protein control) and predetermined protein samples from stimulated primary mouse T cells to define the accuracy and precision of the BOOST method in primary cells (Figure 1A,B). In PV BOOST experiments, there is the potential for reporter ion interference between nearby channels.[40] In our previous study we found evidence of reporter ion interference from channel 126 (+PV) to 127C, however we found no evidence of leakage from 126 to 127N.[21] Therefore, we included a "Blank" channel (127C) to catch potential reporter ion interference from the 1.0 mg PV-treated sample (126; Figure 1B). To enrich for pTyr-containing peptides, we used the superbinder SH2 method[18–20,22] prior to acquisition and analysis by LC-MS and MaxQuant, respectively. To understand how the ΦSDM affects pTyr quantitation in BOOST experiments, our BOOST and control TMT mixes were acquired with (+ΦSDM) and without the ΦSDM on an Orbitrap Eclipse Tribrid mass spectrometer (Figure 1A). From all experiments (BOOST and control, with and without the ΦSDM), the majority of identified phosphorylation sites were localized to tyrosines (70%) with 94.1% of pTyr sites being assigned with probability > 0.75 (Supporting Figure 1).

Disabling ΦSDM Increases pTyr Quantitation Depth

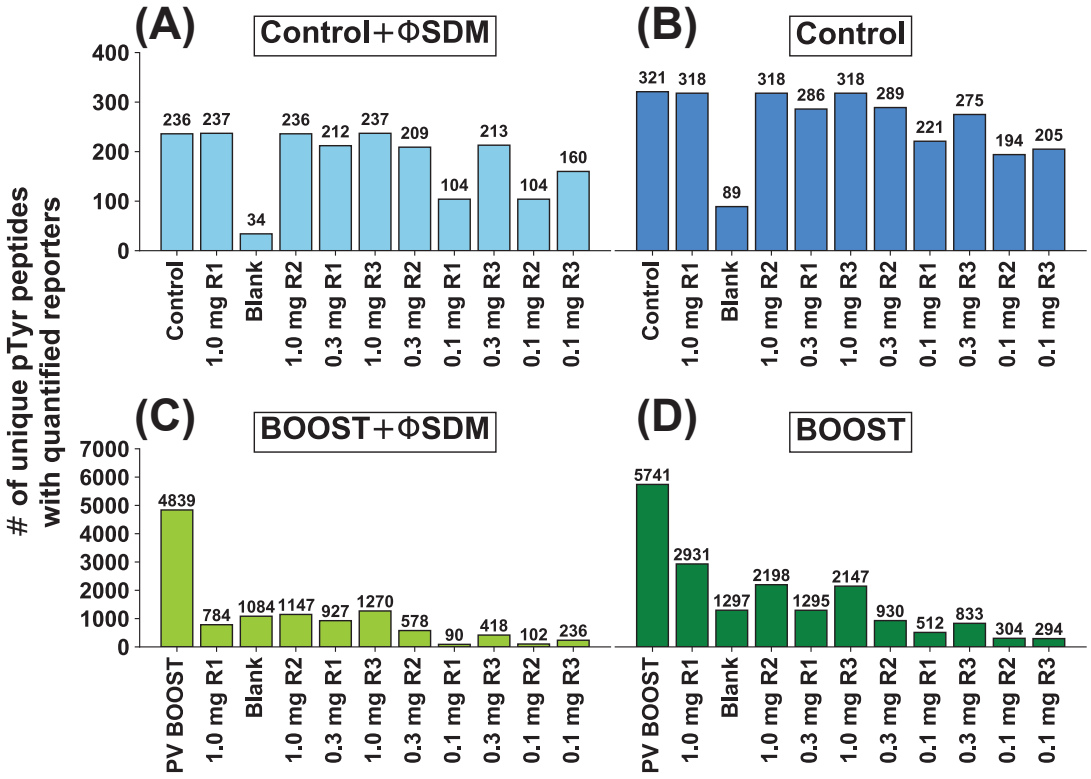

Figure 2: Quantitation depth is improved in BOOST and 1.0 mg Control experiments when the ΦSDM is disabled. The number of unique pTyr peptides identified in each TMT channel for the (A) 1.0 mg Control experiment with the ΦSDM enabled, (B) 1.0 mg Control experiment with the ΦSDM disabled, (C) BOOST experiment with ΦSDM enabled, (D) BOOST experiment with the ΦSDM disabled. The exact number of unique pTyr peptides is indicated above each bar.

To our surprise, disabling the ΦSDM increased the number of pTyr peptides with quantifiable reporters in both the BOOST and control TMT mixes. In the 1.0 mg PV-treated samples, we observed 5,741 unique pTyr peptides with the ΦSDM disabled and only 4,839 with the ΦSDM enabled. On average, 1.0 mg protein input samples using BOOST yielded 2,425 quantifiable pTyr peptides with the ΦSDM disabled compared to 1,067 when the ΦSDM is enabled, a 2.3 fold increase. We observed improvement when disabling the ΦSDM in both 0.3 and 0.1 mg protein input samples in BOOST, with an average of 1,016 and 370 quantifiable pTyr peptides compared to 641 and 143 with the ΦSDM enabled, respectively (Figure 2C,D). The increased quantitation depth also came with more complete data. The

average percentage of missing data for 1.0 mg, 0.3 mg, and 0.1 mg samples using BOOST dropped from 78.4, 87.0, and 97.1 to 59.0, 82.8, and 93.7 when the ΦSDM was disabled, respectively (Supporting Figure 2C,D). While the control samples did benefit from disabling the ΦSDM, the magnitude of improvement was smaller (1.3-fold for 1.0 mg, 1.3-fold for 0.3 mg, and 1.7-fold for 0.1 mg; Figure 2A,B) and the percentage of missing values between replicates were similar (Supporting Figure 2A,B). Importantly, after removing missing values, the median intensities for each replicate TMT channel were consistent and aligned well with their predetermined starting amounts (Supporting Figure 3). The consistency of the reporter intensity values for the 1.0 mg protein samples suggests there was minimal reporter ion interference from the 1.0 mg PV-treated sample (126) into the 1.0 mg R1 sample (127N) and reaffirms our experimental design (Figure 1)

Disabling ΦSDM Increases the Reproducibility, Accuracy, Precision of pTyr Quantitation in Low Abundance Samples

Interestingly, we observed a substantial increase in replicate reproducibility after disabling the ΦSDM in both BOOST and control conditions, especially in low abundance samples. We assessed replicate reproducibility by performing simple least squares regression in a pairwise manner on replicates for 1.0 mg, 0.3 mg, and 0.1 mg protein inputs for BOOST and control experiments acquired with and without the ΦSDM (Figure 3A, Supporting Figures 4-7). When the ΦSDM was disabled, we observed higher average values for the coefficient of determination (r^2), a measure of the linear relationship of between data, in all conditions. This effect was clearest in the low abundance samples, where the average r^2 for BOOST experiments with 0.1 mg of protein increased from 0.527 to 0.775 by disabling the ΦSDM (Figure 3A, Supporting Figures 4, 5). We observed similar results in the control samples, where disabling the ΦSDM increased the r^2 from 0.566 to 0.863 (Figure 3A, Supporting Figures 6, 7). Our data suggest that disabling the ΦSDM increases the linear relationship between replicates and, therefore, replicate reproducibility in both BOOST and control experiments.

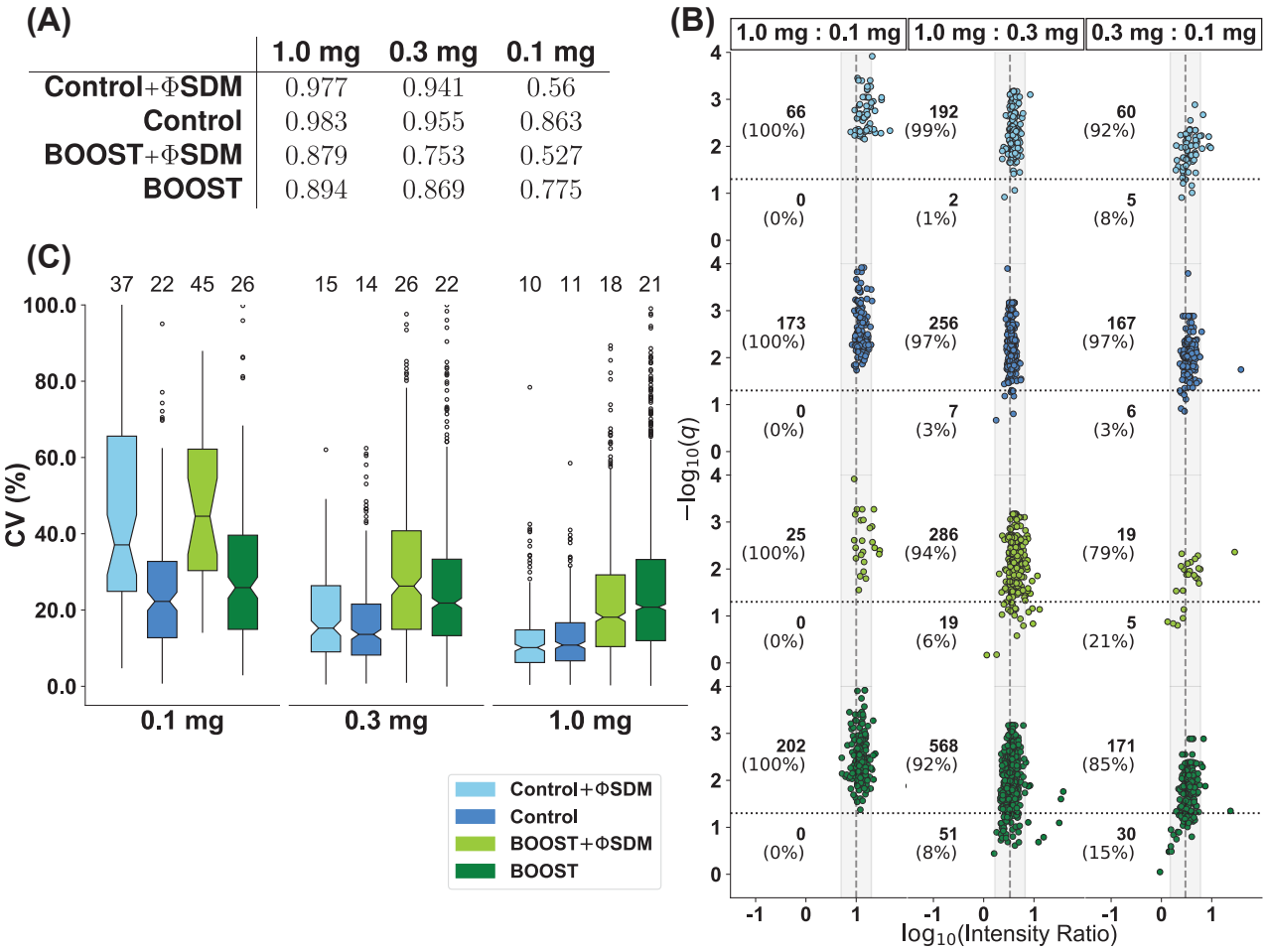

Figure 3: With the ΦSDM disabled, replicate intensity values are more reproducible, more significant ratios of pTyr peptides are observed, and the coefficient of variation for each condition are consistent. (A) Table showing the average coefficient of determination (r^2) from least squares linear regression preformed on replicates. (B) Volcano plot showing contrived ratios for each TMT mix as indicated. The numbers and proportions [in percentages] of ratios above and below a q-value of 0.05 [horizontal black, dotted lines] are indicated. The grey, dashed line indicates the theoretically expected ratio, and the grey shaded area represents 2-fold above and below theoretically expected ratios. (C) Box-and-whisker plots showing the percentage coefficient of variation of the triplicate intensities for each protein input as indicated. The median coefficient of variation percentages are show above each boxplot. Color labels apply to (B) and (C).

In addition to increasing reproducibility, disabling the ΦSDM also increased the accuracy and precision of pTyr quantitaiton. We assessed accuracy by observing clustering around the theoretically expected peptide intensity ratios in volcano plots (Figure 3B). In both the control and BOOST experiments with the ΦSDM disabled, we observed tight clustering of

values around theoretical truth, especially in the 1.0 mg to 0.1 mg comparison. In contrast, enabling the ΦSDM decreased both clustering around the theoretical truth and the number of peptides with a statistically significant difference in mean reporter intensity. Disabling the ΦSDM lead to a 2.8-fold increase in statistically significant ratios between the 0.3 mg and 0.1 mg protein input conditions for control experiments, and a 9.0-fold increase for BOOST experiments (Figure 3B). The increased number of statstically significant ratios with the ΦSDM disabled was coupled with an increase in quantitative precision in low abundance samples. For 0.1 mg protein input samples, disabling the ΦSDM decreased the median coefficient of variation (CV) from 37% to 22% in control experiments and 45% to 26% in BOOST experiments, while the CV% for 0.3 mg and 1.0 mg samples remained similar between control and BOOST experiments (Figure 3C). Together, our data suggest that disabling the ΦSDM for multiplexed TMT experiments with low protein input amounts substantially increases the quality of pTyr quantitation.

The Magnitude of pTyr Quantitation is Improved when ΦSDM is Disabled

Because the goal of BOOST is to improve quantitation of low abundance peptides, we chose to examine the magnitude of improvement with the ΦSDM disabled. We first determined the populations of peptides unique to BOOST ("BOOST-Gained"), unique to the control ("Control-Only"), or found in both experiments ("Overlap") when the ΦSDM was disabled or enabled (Figure 4A,B, Supporting Tables 1-6). While the percentage of BOOST-Gained peptides was high without (90.3%) or with (86.6%) the ΦSDM, we identified 1.94-fold more BOOST-Gained peptides with the ΦSDM disabled than with the ΦSDM enabled (Figure 4A,B). The accuracy of reporter intensity measurements was almost identical in overlapping peptides identified in the BOOST and control experiments with the ΦSDM disabled, with a large increase in the number of significant BOOST-Gained peptides in all contrived ratios (Supporting Figure 8). In contrast, the accuracy and yield of significant overlapping peptides

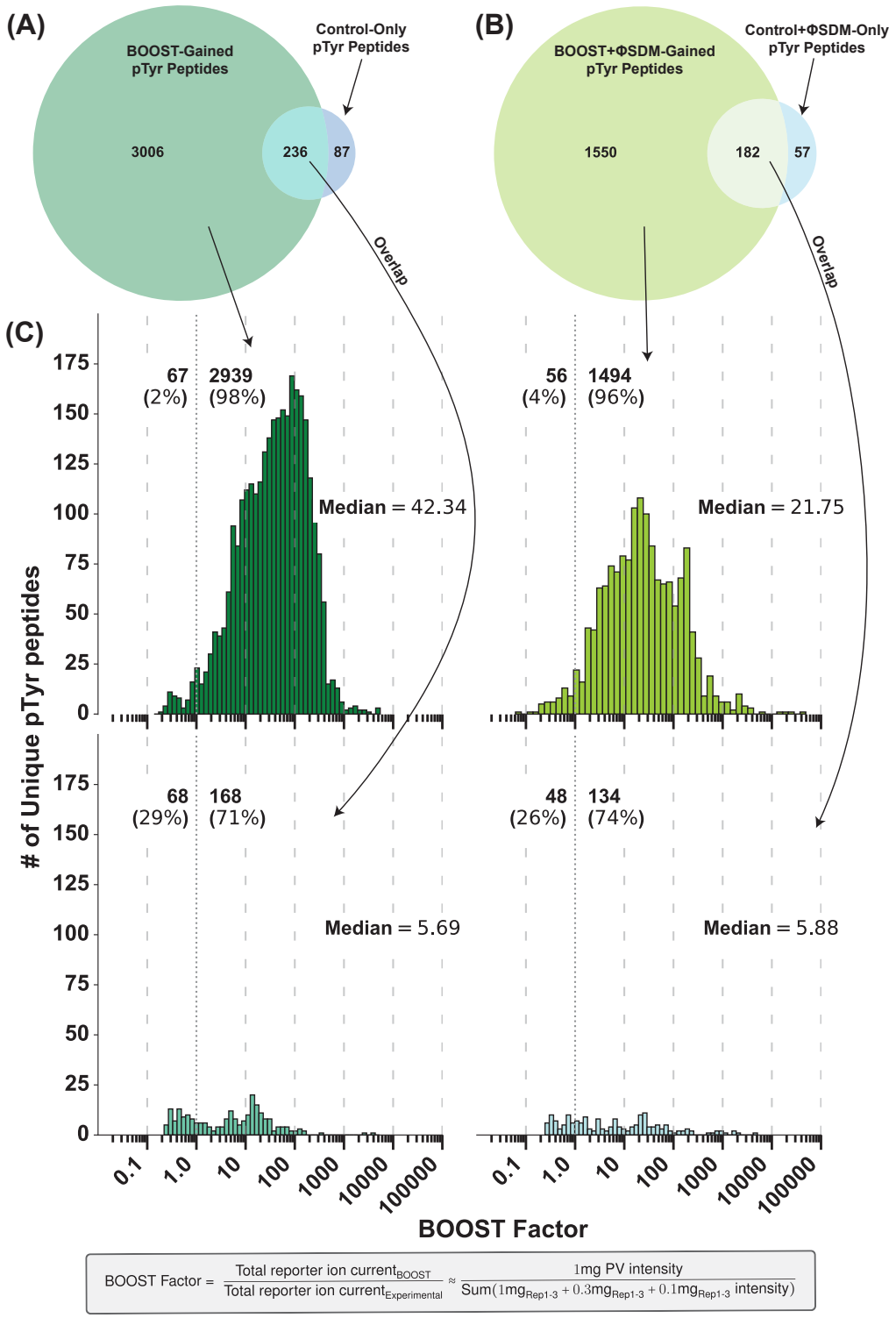

Figure 4: The number of peptides and the magnitude of BOOST factor are increased when the ΦSDM is disabled. (A) Venn diagram showing the number of unique pTyr peptides observed when the ΦSDM is disabled in the BOOST, the 1.0 mg Control, and in both the BOOST and 1.0 mg Control TMT mixes. (B) Venn diagram showing the number of unique pTyr peptides observed when the ΦSDM is disabled in the BOOST, the 1.0 mg Control, and in both the BOOST and 1.0 mg Control TMT mixes.

were severely lowered in the BOOST experiment compared to the control with the ΦSDM enabled (Supporting Figure 9). When comparing the unique pTyr peptides observed in the BOOST experiments with or without the ΦSDM, we found that 56.8% (2278) of the unique pTyr peptides were observed exclusively with the ΦSDM disabled, whereas only 19.2% (768) of pTyr peptides were observed exclusively with the ΦSDM (Supporting Figure 10A). For the control samples, the majority of the unique pTyr peptides were observed both with and without the ΦSDM (48.0%) although disabling the ΦSDM led to a modest increase in the percentage of unique pTyr peptides acquired (37.0% versus 15.0%; Supporting Figure 10B). Our data suggest that the ΦSDM degrades the accuracy of measruements in control-overlapping pTyr peptides and limits the potential to identify unique pTyr peptides.

In our paper describing the BOOST method, we determined the magnitude of quantitative improvement in BOOST experiments using "BOOST factors", defined as the ratio of the reporter intensity from the PV-treated sample to the sum of reporter intensities from experimental channels for a specific peptide (Figure 4C, bottom).[20] A peptide with a BOOST factor exceeding 1 occurs when the reporter ion current of the PV-treated sample is greater than the reporter ion current of the experimental channels, indicating the peptide is generally scarce in the experimental samples.[20] Overall, the majority of BOOST-Gained peptides had BOOST factors greater than 1 regardless of whether the ΦSDM was enabled or disabled. However, disabling ΦSDM shifted the median BOOST factor value from 21.75 to 42.34 (Figure 4C). The overlapping peptides had relatively similar BOOST factor distributions with (median = 5.69) or without (median = 5.88) the ΦSDM, suggesting that BOOST-Gained peptides were lower in abundance with or without the ΦSDM and that disabling the ΦSDM increased acquisition of low abundance peptides. To account for BOOST-Gained pTyr peptides with missing values, we filtered the data to contain pTyr peptides where intensity ratios and statistical significance could be attained and plotted their cumulative distributions (Supporting Figure 11). For low abundance ratios (0.3 mg to 0.1 mg, $n = 92$ and 1.0 mg to 0.1 mg, $n = 115$) acquired without the ΦSDM, 90% of the significantly changing pTyr peptides

had a BOOST factor less than 5, which shifted to about 18 in the higher abundance ratio (1.0 mg to 0.3 mg). For ratios acquired with the ΦSDM enabled, three pTyr peptides with BOOST factors less than 1 had statistically significant ratios for 0.3 mg to 0.1 mg and seven pTyr peptides with BOOST factors less than 5 had statistically significant ratios for 1.0 mg to 0.1 mg (Supporting Figure 11). When we included ratios where at least one replicate value was identified for each protein input sample, the distribution of BOOST factors were almost identical for low abundance samples with 90% of pTyr peptides having BOOST factors less than 20 (Supporting Figure 11). These data suggest that disabling the ΦSDM increases the quantity and quality of low abundance pTyr peptides observed using the BOOST method in primary T cells from mice.

BOOST Reveals pTyr Sites Critical for T cell Receptor Signaling in Primary T cells

Discussion

To improve our understanding of the critical tyrosine phosphorylation events involved in TCR signaling and other cellular processes, accurate methods to perform deep profiling of the pTyr proteome are required. Although the accuracy of LC-MS/MS techniques are desirable for pTyr proteomics, the low abundance of tyrosine phosphorylation events in the proteome hinder the frequently used global phosphoenrichment methods like TiO_2 or IMAC.[10,11,41–43] Although recent developments in pTyr-specific enrichment techniques like p-Tyr-1000 and the superbinder SH2 method have improved pTyr proteomics,[14–20] the issue of low pTyr abundance is apparent when using samples that are difficult or expensive to collect, such as primary cells from humans or mice.[6,8,9] Increasing quantitative yield in low abundance samples has been acheived in multiplexed TMT experiments using a carrier proteome sample,[40,44,45] and we developed the BOOST method using a pervanadate treated sample to increase quantitative yield of pTyr peptides.[20,21]

Here, we demonstrate the first use of the BOOST method in primary T cells from mice, defining the accuracy, precision, and profiling depth of the mouse T cell pTyr proteome in low abundance samples. Our multiplexed TMT experiments were designed to minimize reporter ion interference from the pervanadate channel by including a "Blank" (127C) channel where maximal reporter ion interference has been observed previously.[21,40] Using BOOST, we were able to quantify more than 2,000, 900, and 300 unqiue pTyr peptides in 1.0 mg, 0.3 mg, and 0.1 mg protein samples, respectively (Figure 2D), while maintaining accuracy and precision (Figure 3, Supporting Figure 4). Using BOOST allowed for 3,006 BOOST-gained pTyr peptides to be quantified with 2,939 pTyr peptides that were low abundance in the samples (Figure 4C). Together, our data suggest that including a pervanadate BOOST channel increases quantitative depth of low abundance peptides in higher abundance samples and overall quantitation in low abundance samples without large comprimises to accuracy or precision.

Something about the sites we see in tobias' stuff

We also examined the influence of the acquisition parameter ΦSDM, a computational method that increases acquisition rate of FT-MS by efficient and noise tolerant deconvolution of FT spectra,[29] on our BOOST and 1.0 mg Control samples. Although previous research has shown that using the ΦSDM on long gradients or scarce samples may reduce the efficiency of the algorithm due to low ion currents,[29,46,47] the influence of the ΦSDM on TMT mixes with carrier proteome channels has yet to be evaluated. Our data are in agreement with previous literature suggesting that enabling the ΦSDM degrades low abundance samples. We observed a decrease of about 75 to 100 unique pTyr peptides across our 1.0 mg Control samples with the ΦSDM enabled, with the largest loss in the 0.1 mg R1 sample (221 to 104 unique pTyr peptides; Figure 2A,B). Surprisingly, enabling the ΦSDM degraded the quality of data from BOOST experiments. We observed a large reduction of unique pTyr peptide yield in experimental channels, with the largest difference being 1.0 mg R1 dropping from 2,931 unique pTyr peptides to 784 unique pTyr peptides with the ΦSDM enabled

(Figure 2C,D). We also observed a reduction in accuracy (Figure 3B), precision (Figure 3C), and replicate reproducibility (Supporting Figures 4, 5) with the ΦSDM enabled. Our study indicates that disabling the ΦSDM, or "Turbo-TMT" on the method editor on Orbitrap instruments, subtstantially improves the quantitation depth of low abundance posttranslational modification samples, especially when a BOOST channel is present.

With increased interest in using proteomics to study rare or specific posttranslational modifications[19,48,49] and the proteomes of single-cells,[44,45,50] reliable methods to increase multiplexing capabilities,[51] posttranslational modification selection,[52] and quantitation[20,21,53] are desired. These experimental techniques will come with a wave of computational methods to further improve quantitation,[29,54,55] which will require stringent testing for both experimental-computational method compatibility and to understand the range of biological processes that these methods can work with. In this study, we displayed both of these features for the BOOST method by showing that BOOST and the ΦSDM were incompatible and that BOOST can increase the yield of pTyr peptides in primary T cells from mice, which are notoriously difficult to perform large scale pTyr proteomics experiments on.[6] By using this study as a benchmark for the BOOST method in primary T cells from mice, future research into the pTyr proteome of primary T cells from mice is possible using far less sample than is conventionally used in shotgun proteomics.

Conclusion

Our study defines the accuracy, precision, and profiling depth of multiplexed TMT experiments using a pervandate BOOST channel to increase quantitative yield of pTyr peptides in stimulated primary T cells from mice. We found that including the BOOST channel increases the quantitative yield of unique pTyr peptides without jeoprodizing accuracy, precision, or replicate reproducibility in low abundance samples. The majority of the unique pTyr peptides observed in the BOOST channel and at least one experimental channel were

scarce in the samples, suggesting that BOOST increases identification of rare pTyr peptides. Surprisingly, we found that enabling the ΦSDM degrades the quality of data in BOOST experiments, almost halving the unique pTyr peptide yield and reducing accuracy, precision, and replicate reproducibility in low abundance samples. **Something about the sites we see in tobias' stuff.** Together, our study shows that multiplexed TMT experiments using a pervanadate BOOST channel increase quatitative yield of meaningful unique pTyr peptides in primary T cells from mice and that the ΦSDM should not be used during BOOST experiments.

Supporting Information

The Supporting Information is available free of charge at https://pubs.acs.org/. Supporting Information includes:

- All tables generated after MaxQuant analysis of .raw files ("summary.txt", "evidence.txt", "peptides.txt", "modificationSpecificPeptides.txt", "Oxidation (M)Sites.txt", "Phospho (STY)Sites.txt", "proteinGroups.txt", "allPeptides.txt", "msScans.txt", "mzRange.txt", "msmsScans.txt", and "msms.txt") (.ZIP)
- All Python3 code used to perform data analysis and representation, including statistical analyses, replicate reproducibility assessments, BOOST factor analysis, and comparisons between TMT experiments (.ZIP)
- All output from statistical analyses performed and selected MaxQuant output required for statistical analysis (.XLSX)

Acknowledgements

The authors wish to thank Dr. Ricky Edmondson and Dr. Samuel G. Mackintosh from University of Arkansas for Medical Sciences (UAMS) for collecting the proteomic data. We ac-

knowledge financial support from NIH grants R01AI083636, P20GM121293, and R24GM137786. Kenneth P. Callahan was supported by T32GM136566 and the Sidney E. Frank Fellowship.

Data Availability

The mass spectrometry proteomic data have been deposited to the ProteomeXchange Consortium (http://proteomecentral.proteomexchange.org) via the PRIDE partner repository[56] with the dataset identifier PXD025853 (Username: reviewer_pxd025853ebi.ac.uk , Password: RDtiS7iG).

References

(1) Gaud, G.; Lesourne, R.; Love, P. E. Regulatory mechanisms in T cell receptor signalling. *Nature Reviews Immunology* **2018**, *18*, 485–497.

(2) Palacios, E. H.; Weiss, A. Function of the Src-family kinases, Lck and Fyn, in T-cell development and activation. *Oncogene* **2004**, *23*, 7990–8000.

(3) Lo, W.-L.; Shah, N. H.; Ahsan, N.; Horkova, V.; Stepanek, O.; Salomon, A. R.; Kuriyan, J.; Weiss, A. Lck promotes Zap70-dependent LAT phosphorylation by bridging Zap70 to LAT. *Nature immunology* **2018**, *19*, 733–741.

(4) Hunter, T.; Sefton, B. M. Transforming gene product of Rous sarcoma virus phosphorylates tyrosine. *Proceedings of the National Academy of Sciences* **1980**, *77*, 1311–1315.

(5) Hunter, T. Tyrosine phosphorylation: thirty years and counting. *Current opinion in cell biology* **2009**, *21*, 140–146.

(6) Locard-Paulet, M.; Voisinne, G.; Froment, C.; Goncalves Menoita, M.; Ounoughene, Y.; Girard, L.; Gregoire, C.; Mori, D.; Martinez, M.; Luche, H., et al. LymphoAtlas: a dynamic and integrated phosphoproteomic resource of TCR signaling in primary T

cells reveals ITSN 2 as a regulator of effector functions. *Molecular systems biology* **2020**, *16*, e9524.

(7) Joshi, R. N.; Binai, N. A.; Marabita, F.; Sui, Z.; Altman, A.; Heck, A. J.; Tegnér, J.; Schmidt, A. Phosphoproteomics reveals regulatory T cell-mediated DEF6 dephosphorylation that affects cytokine expression in human conventional T cells. *Frontiers in immunology* **2017**, *8*, 1163.

(8) Salter, A. I.; Rajan, A.; Kennedy, J. J.; Ivey, R. G.; Shelby, S. A.; Leung, I.; Templeton, M. L.; Muhunthan, V.; Voillet, V.; Sommermeyer, D.; Whiteaker, J. R.; Gottardo, R.; Veatch, S. L.; Paulovich, A. G.; Riddell, S. R. Comparative analysis of TCR and CAR signaling informs CAR designs with superior antigen sensitivity and in vivo function. *Science Signaling* **2021**, *14*, eabe2606.

(9) Ramello, M. C.; Benzaïd, I.; Kuenzi, B. M.; Lienlaf-Moreno, M.; Kandell, W. M.; Santiago, D. N.; Pabón-Saldaña, M.; Darville, L.; Fang, B.; Rix, U.; Yoder, S.; Berglund, A.; Koomen, J. M.; Haura, E. B.; Abate-Daga, D. An immunoproteomic approach to characterize the CAR interactome and signalosome. *Science Signaling* **2019**, *12*, eaap9777.

(10) Navarro, M. N.; Goebel, J.; Feijoo-Carnero, C.; Morrice, N.; Cantrell, D. A. Phosphoproteomic analysis reveals an intrinsic pathway for the regulation of histone deacetylase 7 that controls the function of cytotoxic T lymphocytes. *Nature immunology* **2011**, *12*, 352–361.

(11) Prado, D. S.; Cattley, R. T.; Shipman, C. W.; Happe, C.; Lee, M.; Boggess, W. C.; MacDonald, M. L.; Hawse, W. F. Synergistic and additive interactions between receptor signaling networks drive the regulatory T cell versus T helper 17 cell fate choice. *Journal of Biological Chemistry* **2021**, *297*.

(12) Iwai, L. K.; Benoist, C.; Mathis, D.; White, F. M. Quantitative Phosphoproteomic

Analysis of T Cell Receptor Signaling in Diabetes Prone and Resistant Mice. *Journal of Proteome Research* **2010**, *9*, 3135–3145, PMID: 20438120.

(13) Álvarez-Salamero, C.; Castillo-González, R.; Pastor-Fernández, G.; Mariblanca, I. R.; Pino, J.; Cibrian, D.; Navarro, M. N. IL-23 signaling regulation of pro-inflammatory T-cell migration uncovered by phosphoproteomics. *PLoS biology* **2020**, *18*, e3000646.

(14) Kaneko, T.; Huang, H.; Cao, X.; Li, X.; Li, C.; Voss, C.; Sidhu, S. S.; Li, S. S. Superbinder SH2 domains act as antagonists of cell signaling. *Science signaling* **2012**, *5*, ra68–ra68.

(15) Bian, Y.; Li, L.; Dong, M.; Liu, X.; Kaneko, T.; Cheng, K.; Liu, H.; Voss, C.; Cao, X.; Wang, Y., et al. Ultra-deep tyrosine phosphoproteomics enabled by a phosphotyrosine superbinder. *Nature chemical biology* **2016**, *12*, 959–966.

(16) Dong, M.; Bian, Y.; Wang, Y.; Dong, J.; Yao, Y.; Deng, Z.; Qin, H.; Zou, H.; Ye, M. Sensitive, robust, and cost-effective approach for tyrosine Phosphoproteome analysis. *Analytical chemistry* **2017**, *89*, 9307–9314.

(17) Tong, J.; Cao, B.; Martyn, G. D.; Krieger, J. R.; Taylor, P.; Yates, B.; Sidhu, S. S.; Li, S. S.; Mao, X.; Moran, M. F. Protein-phosphotyrosine proteome profiling by superbinder-SH2 domain affinity purification mass spectrometry, sSH2-AP-MS. *Proteomics* **2017**, *17*, 1600360.

(18) Yao, Y.; Bian, Y.; Dong, M.; Wang, Y.; Lv, J.; Chen, L.; Wang, H.; Mao, J.; Dong, J.; Ye, M. SH2 Superbinder modified monolithic capillary column for the sensitive analysis of protein tyrosine phosphorylation. *Journal of proteome research* **2018**, *17*, 243–251.

(19) Yao, Y.; Wang, Y.; Wang, S.; Liu, X.; Liu, Z.; Li, Y.; Fang, Z.; Mao, J.; Zheng, Y.; Ye, M. One-step SH2 superbinder-based approach for sensitive analysis of tyrosine phosphoproteome. *Journal of proteome research* **2019**, *18*, 1870–1879.

(20) Chua, X. Y.; Mensah, T.; Aballo, T.; Mackintosh, S. G.; Edmondson, R. D.; Salomon, A. R. Tandem mass tag approach utilizing pervanadate BOOST channels delivers deeper quantitative characterization of the tyrosine phosphoproteome. *Molecular & Cellular Proteomics* **2020**, *19*, 730–743.

(21) Chua, X. Y.; Salomon, A. Ovalbumin Antigen-Specific Activation of Human T Cell Receptor Closely Resembles Soluble Antibody Stimulation as Revealed by BOOST Phosphotyrosine Proteomics. *Journal of Proteome Research* **2021**, 10.1021/acs.jproteome.1c00239.

(22) Griffith, A. A.; Callahan, K. P.; King, N. G.; Xiao, Q.; Su, X.; Salomon, A. R. SILAC phosphoproteomics reveals unique signaling circuits in CAR-T cells and the inhibition of B cell-activating phosphorylation in target cells. *Journal of proteome research* **2021**, 10.1021/acs.jproteome.1c00735.

(23) Thompson, A.; Schäfer, J.; Kuhn, K.; Kienle, S.; Schwarz, J.; Schmidt, G.; Neumann, T.; Hamon, C. Tandem mass tags: a novel quantification strategy for comparative analysis of complex protein mixtures by MS/MS. *Analytical chemistry* **2003**, *75*, 1895–1904.

(24) Wiese, S.; Reidegeld, K. A.; Meyer, H. E.; Warscheid, B. Protein labeling by iTRAQ: a new tool for quantitative mass spectrometry in proteome research. *Proteomics* **2007**, *7*, 340–350.

(25) Werner, T.; Becher, I.; Sweetman, G.; Doce, C.; Savitski, M. M.; Bantscheff, M. High-resolution enabled TMT 8-plexing. *Analytical chemistry* **2012**, *84*, 7188–7194.

(26) McAlister, G. C.; Huttlin, E. L.; Haas, W.; Ting, L.; Jedrychowski, M. P.; Rogers, J. C.; Kuhn, K.; Pike, I.; Grothe, R. A.; Blethrow, J. D., et al. Increasing the multiplexing capacity of TMTs using reporter ion isotopologues with isobaric masses. *Analytical chemistry* **2012**, *84*, 7469–7478.

(27) O'Connell, J. D.; Paulo, J. A.; O'Brien, J. J.; Gygi, S. P. Proteome-wide evaluation of two common protein quantification methods. *Journal of proteome research* **2018**, *17*, 1934–1942.

(28) Thompson, A.; Wölmer, N.; Koncarevic, S.; Selzer, S.; Böhm, G.; Legner, H.; Schmid, P.; Kienle, S.; Penning, P.; Hoöhle, C., et al. TMTpro: design, synthesis, and initial evaluation of a proline-based isobaric 16-plex tandem mass tag reagent set. *Analytical chemistry* **2019**, *91*, 15941–15950.

(29) Grinfeld, D.; Aizikov, K.; Kreutzmann, A.; Damoc, E.; Makarov, A. Phase-constrained spectrum deconvolution for Fourier transform mass spectrometry. *Analytical chemistry* **2017**, *89*, 1202–1211.

(30) Abraham, R. T.; Weiss, A. Jurkat T cells and development of the T-cell receptor signalling paradigm. *Nature reviews immunology* **2004**, *4*, 301–308.

(31) Wiśniewski, J. R.; Zougman, A.; Nagaraj, N.; Mann, M. Universal sample preparation method for proteome analysis. *Nature methods* **2009**, *6*, 359–362.

(32) Ahsan, N.; Salomon, A. R. *The Immune Synapse*; Springer, 2017; pp 369–382.

(33) McAlister, G. C.; Nusinow, D. P.; Jedrychowski, M. P.; Wuühr, M.; Huttlin, E. L.; Erickson, B. K.; Rad, R.; Haas, W.; Gygi, S. P. MultiNotch MS3 enables accurate, sensitive, and multiplexed detection of differential expression across cancer cell line proteomes. *Analytical chemistry* **2014**, *86*, 7150–7158.

(34) Cox, J.; Mann, M. MaxQuant enables high peptide identification rates, individualized ppb-range mass accuracies and proteome-wide protein quantification. *Nature biotechnology* **2008**, *26*, 1367–1372.

(35) Cox, J.; Neuhauser, N.; Michalski, A.; Scheltema, R. A.; Olsen, J. V.; Mann, M. An-

dromeda: a peptide search engine integrated into the MaxQuant environment. *Journal of proteome research* **2011**, *10*, 1794–1805.

(36) Hornbeck, P. V.; Zhang, B.; Murray, B.; Kornhauser, J. M.; Latham, V.; Skrzypek, E. PhosphoSitePlus, 2014: mutations, PTMs and recalibrations. *Nucleic acids research* **2015**, *43*, D512–D520.

(37) Martens, M.; Ammar, A.; Riutta, A.; Waagmeester, A.; Slenter, D. N.; Hanspers, K.; A. Miller, R.; Digles, D.; Lopes, E. N.; Ehrhart, F., et al. WikiPathways: connecting communities. *Nucleic acids research* **2021**, *49*, D613–D621.

(38) Benjamini, Y.; Hochberg, Y. Controlling the false discovery rate: a practical and powerful approach to multiple testing. *Journal of the Royal statistical society: series B (Methodological)* **1995**, *57*, 289–300.

(39) Grus, J. *Data Science from Scratch: Sirst Principles with Python*; O'Reilly Media, 2019.

(40) Stopfer, L. E.; Conage-Pough, J. E.; White, F. M. Quantitative consequences of protein carriers in immunopeptidomics and tyrosine phosphorylation MS2 analyses. *Molecular & Cellular Proteomics* **2021**, *20*.

(41) Thingholm, T. E.; Jørgensen, T. J.; Jensen, O. N.; Larsen, M. R. Highly selective enrichment of phosphorylated peptides using titanium dioxide. *Nature protocols* **2006**, *1*, 1929–1935.

(42) Thingholm, T. E.; Larsen, M. R. *Phospho-Proteomics*; Springer, 2016; pp 135–146.

(43) Thingholm, T. E.; Larsen, M. R. *Phospho-Proteomics*; Springer, 2016; pp 123–133.

(44) Petelski, A. A.; Emmott, E.; Leduc, A.; Huffman, R. G.; Specht, H.; Perlman, D. H.; Slavov, N. Multiplexed single-cell proteomics using SCoPE2. *Nature protocols* **2021**, *16*, 5398–5425.

(45) Cheung, T. K.; Lee, C.-Y.; Bayer, F. P.; McCoy, A.; Kuster, B.; Rose, C. M. Defining the carrier proteome limit for single-cell proteomics. *Nature Methods* **2021**, *18*, 76–83.

(46) Yu, Q.; Paulo, J. A.; Naverrete-Perea, J.; McAlister, G. C.; Canterbury, J. D.; Bailey, D. J.; Robitaille, A. M.; Huguet, R.; Zabrouskov, V.; Gygi, S. P., et al. Benchmarking the orbitrap tribrid eclipse for next generation multiplexed proteomics. *Analytical chemistry* **2020**, *92*, 6478–6485.

(47) Kelstrup, C. D.; Aizikov, K.; Batth, T. S.; Kreutzman, A.; Grinfeld, D.; Lange, O.; Mourad, D.; Makarov, A. A.; Olsen, J. V. Limits for resolving isobaric tandem mass tag reporter ions using phase-constrained spectrum deconvolution. *Journal of proteome research* **2018**, *17*, 4008–4016.

(48) Millan-Ariño, L.; Yuan, Z.-F.; Oomen, M. E.; Brandenburg, S.; Chernobrovkin, A.; Salignon, J.; Körner, L.; Zubarev, R. A.; Garcia, B. A.; Riedel, C. G. Histone Purification Combined with High-Resolution Mass Spectrometry to Examine Histone Post-Translational Modifications and Histone Variants in Caenorhabditis elegans. *Current Protocols in Protein Science* **2020**, *102*, e114.

(49) Fulzele, A.; Bennett, E. J. *The Ubiquitin Proteasome System*; Springer, 2018; pp 363–384.

(50) Vistain, L. F.; Tay, S. Single-cell proteomics. *Trends in Biochemical Sciences* **2021**, *46*, 661–672.

(51) Arul, A. B.; Robinson, R. A. Sample multiplexing strategies in quantitative proteomics. *Analytical chemistry* **2018**, *91*, 178–189.

(52) Pieroni, L.; Iavarone, F.; Olianas, A.; Greco, V.; Desiderio, C.; Martelli, C.; Manconi, B.; Sanna, M. T.; Messana, I.; Castagnola, M., et al. Enrichments of post-translational modifications in proteomic studies. *Journal of separation science* **2020**, *43*, 313–336.

(53) Pino, L. K.; Just, S. C.; MacCoss, M. J.; Searle, B. C. Acquiring and analyzing data independent acquisition proteomics experiments without spectrum libraries. *Molecular & Cellular Proteomics* **2020**, *19*, 1088–1103.

(54) Sinitcyn, P.; Hamzeiy, H.; Salinas Soto, F.; Itzhak, D.; McCarthy, F.; Wichmann, C.; Steger, M.; Ohmayer, U.; Distler, U.; Kaspar-Schoenefeld, S., et al. MaxDIA enables library-based and library-free data-independent acquisition proteomics. *Nature biotechnology* **2021**, *39*, 1563–1573.

(55) Bilbao, A.; Gibbons, B. C.; Slysz, G. W.; Crowell, K. L.; Monroe, M. E.; Ibrahim, Y. M.; Smith, R. D.; Payne, S. H.; Baker, E. S. An algorithm to correct saturated mass spectrometry ion abundances for enhanced quantitation and mass accuracy in omic studies. *International journal of mass spectrometry* **2018**, *427*, 91–99.

(56) Vizcaíno, J. A.; Côté, R. G.; Csordas, A.; Dianes, J. A.; Fabregat, A.; Foster, J. M.; Griss, J.; Alpi, E.; Birim, M.; Contell, J., et al. The PRoteomics IDEntifications (PRIDE) database and associated tools: status in 2013. *Nucleic acids research* **2012**, *41*, D1063–D1069.

TOC Graphic